deuteration sensitive vibrations in BChl would be helpful in assigning its vibrations to a first approximation.

The effect of deuteration on the RR spectrum of BChl may be seen by comparing the spectrum in Figure 7a (fully protonated) with that in Figure 7b (fully deuterated). Both spectra were obtained on dry films. As may be seen, large differences exist between the two spectra and it is difficult in some cases to correlate the bands. Caution must be exercised as discussed in the case of Cu porphin where deuteration was found to produce either a decrease in a particular vibrational frequency (due to the pure isotope effect) or an increase in its value (because of a change in composition or form of the normal mode). With this caveat in mind, bands most sensitive to deuteration are tentatively identified as follows: 1609 (-12), 1589 (-51), 1286 (-26 or -47) (where the number given is the value (cm^{-1}) for the fully protonated form and the number in parentheses is the direction and magnitude of the shift on deuteration). A more detailed analysis of the effects of deuteration is underway.

Conclusions

The resonance Raman results presented here indicate that it is possible to distinguish certain types of BChl interactions through changes in its spectrum. In monomeric BChl systems, the most easily distinguished are coordination interactions. Two structure sensitive bands have been identified, band A (1609 cm^{-1}) and band B (1529 cm^{-1}). (A shoulder on band A near 1589 cm^{-1} is also sensitive to coordination, but it is not well resolved.) The formation of six-coordinate BChl, through the interaction of two ligands at the central Mg atom, causes band A to shift 15-cm^{-1} to lower frequencies and band B to split into two bands of equal intensity (1530 and 1519 cm^{-1}). These changes are consistent with the core expansion correlation[27] which has been invoked to explain similar shifts in structure sensitive bands in a variety of porphyrins. In BChl the movement of its Mg atom into the plane of the macrocycle with an increase in coordination number should lead to an expansion of the porphyrin core. This expansion, in turn, results in an increase in bond length and a decrease in vibrational frequencies for those modes which are most affected (i.e., the methine C=C and pyrrole C=N stretching modes). In aggregated BChl systems, it has been observed that substantial differences are present in the RR spectra with respect to monomeric BChl, as well as between two of the three types of aggregates studied. In the pyrazine aggregate, formed through bifunctional coordination of pyrazine to Mg in BChl, both bands A and B indicate BChl is six-coordinate. Differences which are present between the RR spectrum of this aggregate and monomeric six-coordinate BChl include an enhancement of low-frequency modes between 600 and 700 cm^{-1}, which either are not observed or are extremely weak in monomeric BChl spectra, and an enhancement of the 1341-cm^{-1} mode. The RR spectrum of a second type of aggregate, the BChl hydrate, is distinctive from both that of monomeric BChl and the pyrazine adduct. Both bands A and B are split, and band B is shifted to higher frequencies as compared to those of monomeric BChl. Shoulders on band A at 1637 and 1627 cm^{-1} are characteristic of hydrogen-bonded C=O vibrations (the C-2 acetyl and C-9 keto). Hydrogen bonding of the C=O appears to enhance their RR scattering, perhaps through an increase in conjugation with the porphyrin π systems.[28]

BChl interactions which produced much smaller changes in its RR spectrum include hydrogen bonding in monomeric solutions and self-aggregation. Hydrogen bonding in EtOH caused only a shift in the weak 1675-cm^{-1} acetyl C=O band. Self-aggregation produced changes only in the relative intensities of the bands, especially that at 1609 cm^{-1}, resulting primarily from C=C stretching vibrations of the methines. It is possible, however, that greater effects in the RR spectrum of BChl as a result of hydrogen bonding or self-aggregation might be observed by using a different laser excitation wavelength. For example, excitation close in resonance with the Soret absorption bands produces stronger C=O scattering and would be more useful for studying hydrogen-bonding interactions.

In summary, the RR results discussed above are encouraging with respect to its potential application to the study of BChl interactions in vivo. Although reaction center and BChl protein complexes have already been examined by this technique,[29] the effect of defined BChl interactions in vitro on its RR spectrum has not been examined in detail.[30]

Acknowledgment. The authors wish to express their appreciation for financial support from NIH (Grant 5R01 GM27498). T.M.C. acknowledges support from the donors of the Petroleum Research Fund, administered by the American Chemical Society, and Research Corporation. The deuterated BChl sample was provided by Dr. Marion Thurnauer.

(27) Spaulding, L. D.; Chang, C. C.; Yu, N. T.; Felton, R. H. *J. Am. Chem. Soc.* **1975**, *97*, 2517-2525. Felton, R. H.; Yu, N. T.; O'Shea, D. C.; Shulnutt, J. A. *Ibid.* **1974**, *96*, 3675-3676.

(28) Hirakawa, A. Y.; Tsuboi, M. *Science (Washington, D.C.)* **1975**, *188*, 359-362.

(29) Lutz, M. "Proceedings of the 7th International Conference on Raman Spectroscopy", Aug 4-9, 1980.

(30) Lutz has investigated some of the effects of BChl interactions on its RR spectrum in ref 10b.

Secondary Ion Mass Spectrometry of Small-Molecule Solids at Cryogenic Temperatures. 2.[1] Rare Gas Solids

Robert G. Orth, Harry T. Jonkman, David H. Powell, and Josef Michl*

Contribution from the Department of Chemistry, University of Utah, Salt Lake City, Utah 84112. *Received March 11, 1981*

Abstract: Secondary ion mass spectra of neat solid argon, krypton, and xenon were measured as a function of the nature and energy of the primary ions, He^+-Xe^+. With primary ions of large momentum, considerable quantities of large cluster ions of the matrix material are produced.

In secondary ion mass spectrometry (SIMS), the surface of a solid is bombarded by a beam of primary ions and the positive or negative secondary ions emitted from the solid are analyzed by a mass spectrometer. SIMS has been a very useful tool for examining surfaces as well as the bulk of metallic and ionic solids.[2] More recently, its utility for molecular solids of low volatility has begun to be explored.[3,4] Recently, it was also used to obtain the

(1) Part 1: H. T. Jonkman and J. Michl, *J. Am. Chem .Soc.*, **103**, 733, (1981).

0002-7863/81/1503-6026$01.25/0

mass spectrum of a compound isolated in argon matrix.[5,6] The wide-ranging potential of the method is becoming generally recognized and has been summarized recently.[7]

In view of these developments, it is unfortunate that little is known with certainty about the fundamental processes involved in the formation of secondary ions and their subsequent emission. It appears to us that in addition to theoretical work[8] it would be helpful to obtain SIMS results on solids composed of very simple molecules with simple fragmentation patterns, and this represents the subject of the present series of investigations.

In the present paper, we report our observations on rare gas solids. They provide the simplest examples of "molecular solids", particularly well suited for theoretical investigations, and are of interest as commonly used matrix materials for stabilization of reactive intermediates. If matrix isolation SIMS is to become a viable technique, the behavior of pure matrix materials clearly needs to be understood.

Experimental Section

The secondary ionization mass spectrometer was constructed of 304 stainless steel and is bakeable up to 200 °C (a cross section of the instrument is shown in ref 1). The ion gun is a Riber model CI-50R which is designed to provide ion beam densities from 10^{-11} amps cm^{-2} to 10^{-3} amps cm^{-2} in the ion energy range of 500 eV to 5 keV. The ion gun is provided with a 2 mm diameter aperture between the gun vessel and the sample chamber through which the ion beam travels. This allows for the use of an efficient differentially pumped system such that pressures in the sample chamber can be maintained in the 10^{-9} torr region while the ion gun is in use. The ion gun vessel is pumped with 100 L/s Pfeiffer Turbomolecular pump which results in a base pressure in the 10^{-9} torr region. The sample chamber is pumped by a sorption pump (10^{-3} torr) followed by a 500 L/s Varian Vac-Ion pump with a base pressure of the order of 10^{-9} torr without baking. The secondary ion mass spectra were obtained with an Extranuclear Laboratories quadrupole mass spectrometer equipped with an electrostatic Bessel box which acts as an energy prefilter. This energy analyzer selects a range of energies of the emitted secondary ions before injecting them into the quadrupole mass filter. The energy the analyzer selects can be varied between 0 and +50 eV for both positive and negative ions and allows one to obtain secondary ion energy distributions. The observed secondary ion energies contain an unknown additive constant due to biasing by the electron floodgun filament. Changing the bias causes a 1–2 eV displacement of the observed intensity distribution curves but does not affect their shapes. The full width at half maximum for the selected energy can be varied between 0.7 and 0.4 eV. The quadrupole mass filter with the Extranuclear high Q head Model 14 allows for a mass range of from 2–1000 amu. With other high Q heads the mass resolution can be improved but the mass range is decreased. The primary ion beam was varied between He^+, Ne^+, Ar^+, Kr^+, and Xe^+. The beams were produced by filling the ion gun vessel with the appropriate research grade gas at a pressure of 8×10^{-7} torr as read from an ion gauge attached to the vessel. The ions were formed by 50 eV electrons, using emission currents between 1 and 20 mA depending on the gas used. Under these conditions, few doubly charged ions are formed (none with He and Ne). With the ion gun operating under these conditions, projectile ion densities striking the target sample were maintained within the range from 1×10^{-8} to 3×10^{-8} A cm^{-2}.

The solid samples were formed by depositing the appropriate gas through a leak valve onto a copper sample plate attached to the cold end of an Air Products cryostat and maintained at a temperature of approximately 18 K. The gas samples were research grade (Matheson) and were not purified further except by freeze and thaw cycles in the introduction chamber. During the desorption, the sample chamber was maintained at a pressure of 10^{-6}–10^{-5} torr. The sample thickness on the sample plate was greater than 10 000 monolayers, which allowed the examination of the matrix without interference from the copper surface.

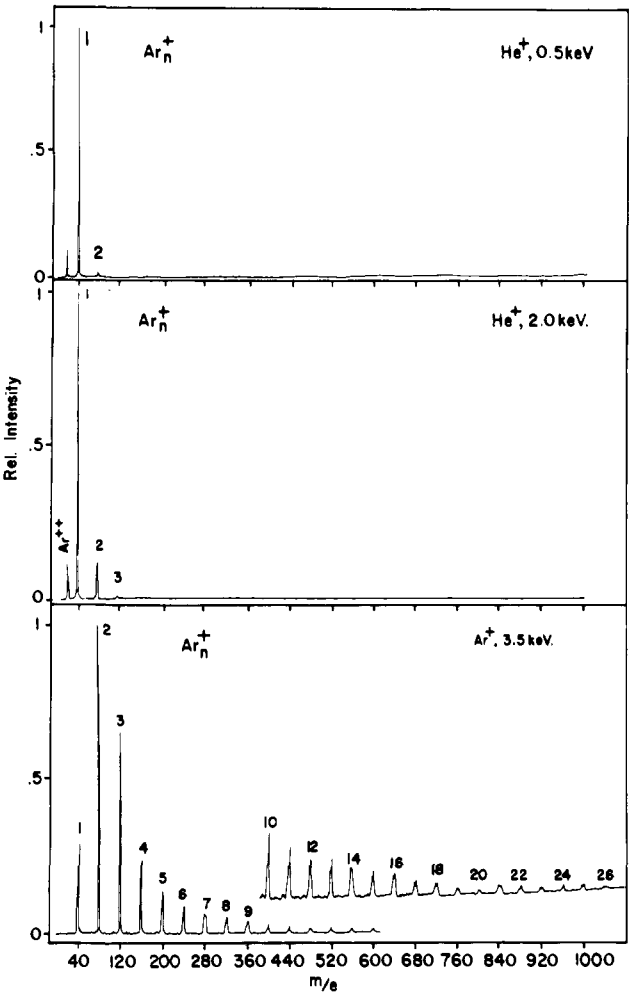

Figure 1. Positive SIMS of solid argon matrix (18 K) with He^+ as the primary ion at impacting energies of 0.5 keV and 2.0 keV, and Ar^+ as the impacting ion at an energy of 3.5 keV.

Since the solid samples were insulators they were flooded with low-energy electrons during the measurement in order to offset the surface charge buildup due to the sputtering by the primary ions. The electrons were provided by an electron flood gun biased at −5 V which provided electron emission currents of up to several mA by adjusting the current through a tungsten filament. It was observed that the overflooding or underflooding of the sample surface with electrons caused dramatic changes in the observed spectra. As might be expected, underflooding caused a loss of intensity, whereas overflooding caused a shift of the relative intensities of peaks in the spectra. It was also noted that the process of maximizing the secondary ion currents by adjustment of the current through the flood gun filament led to varying relative mass intensities when maximizing on ions of different masses. In general, it was observed that when the intensity of the secondary ion current for the monatomic ion was maximixed with use of the flood gun, cluster intensities were either very small or unobservable. This is reasonable considering that the cluster ions are ejected with smaller kinetic energy, as shown later. This effect, and a different design of the flood gun, may well be among the reasons why observed intensities of ion clusters were very low in our original work on molecular solids such as benzene[6] and quite high in the more recent work in this laboratory[1,9] and others.[10] In the present work, the flooding of the surface was always adjusted by monitoring a cluster ion, if available, and maximizing the current due to this secondary ion. This was found to give consistent relative mass intensities.

Results

The secondary ion mass spectra are illustrated in Figure 1, which shows the SIMS of an argon matrix for 0.5 keV and 2 keV

(2) H. W. Werner, in "Electron and Ion Spectroscopy of Solids", L. Fuermans, J. Vennik, and W. Dekeyser, Eds., Plenum, New York, 1978, p 324; P. H. Dawson, *Surface Sci.*, **71**, 247 (1978); **65**, 41 (1977).
(3) A. Benninghoven, *Surface Sci.*, **35**, 427 (1973).
(4) A. Benninghoven, Ed., "Springer Series in Chemical Physics 9, Secondary Ion Mass Spectrometry II", Springer-Verlag, New York, 1979.
(5) H. T. Jonkman and J. Michl, *J. Chem. Soc., Chem. Commun.*, 751 (1978).
(6) H. T. Jonkman, J. Michl, R. N. King, and J. D. Andrade, *Anal. Chem.*, **50**, 2078 (1978).
(7) R. J. Day, S. E. Unger, and R. G. Cooks, *Anal. Chem.*, **52**, 557A (1980).
(8) N. Winograd and B. J. Garrison, *Acc. Chem. Res.*, **13**, 406 (1980).
(9) H. T. Jonkman and J. Michl, "Springer Series in Chemical Physics 9, Secondary Ion Mass Spectrometry II", A. Benninghoven, Ed., Springer-Verlag, New York, 1979, p 292.
(10) G. M. Lancaster, F. Honda, Y. Fukuda, and J. W. Rabalais, *J. Am. Chem. Soc.*, **101**, 1951 (1979).

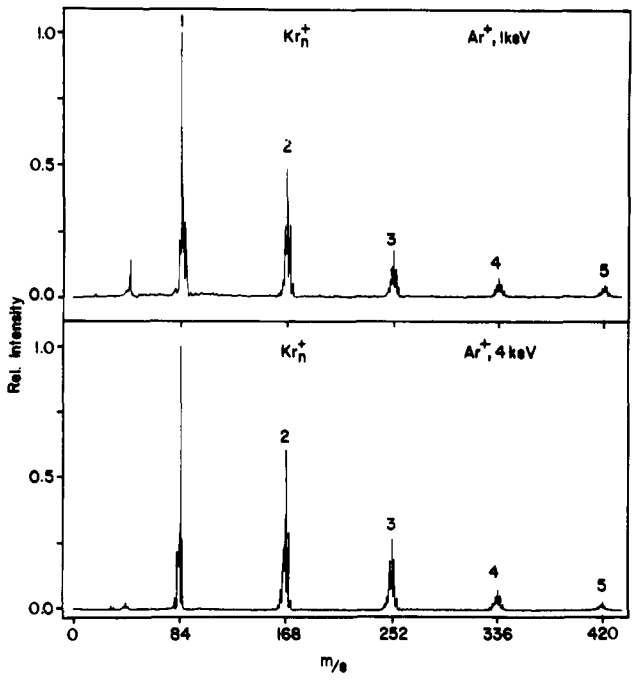

Figure 2. Positive SIMS of solid krypton (18 K) over mass range of 500, using Ar^+ primary ions at kinetic energies of 1 keV and 4 keV.

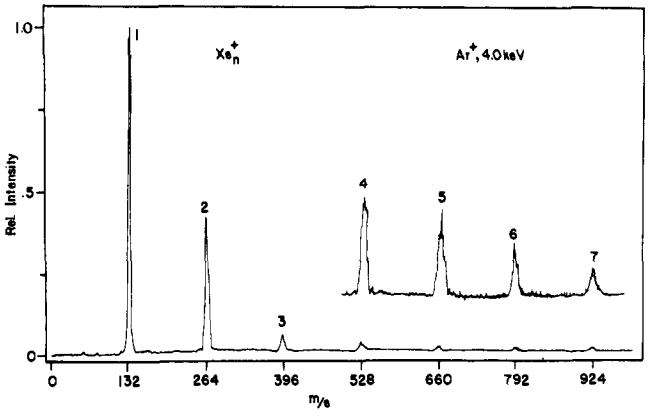

Figure 3. Positive SIMS (low resolution mass scan) of xenon (18 K) with Ar^+ primary ions at 4.0 keV impacting energy.

He^+ and 3.5 keV Ar^+ primary ions, in Figure 2, which shows the SIMS of a krypton matrix for Ar^+ primary ions at 1 keV and 4 keV energies, and in Figure 3, which shows the SIMS of a xenon matrix for Ar^+ primary ions at 4 keV energy.

The spectra contain the expected peaks of the singly charged and, with less intensity, doubly charged monoatomic rare gas ion. The relative abundance of the latter is a sensitive function of the nature of the primary ion but appears to be little affected by its impact energy within the range 0.5–4.0 keV (Figure 1). The solid Ar matrix yields Ar^{2+} with the He^+ and, weakly, with Ne^+ bombardment. Solid Kr and Xe matrices yield Kr^{2+} and Xe^{2+}, respectively, with He^+, Ne^+, and Ar^+ bombardment.

In addition to monoatomic ions, the mass spectra contain cluster ion peaks, whose relative intensity increases as the primary ion is changed in the series $He^+ \cdots Xe^+$ and as its impact energy is increased. The largest clusters observed were Ar_{25}^+, Kr_{12}^+, and Xe_7^+, the limit being the range of our mass spectrometer. The relative intensities of cluster ions Ar_n^+ decrease exponentially with increasing n as noted in previous experiments on other solids,[1,10] except for Ar_{20}^+ which shows a relatively smaller intensity. A more quantitative evaluation is difficult because the transmission of the quadrupole is uneven as a function of mass. Also, it should be noted that our energy filter mounted in front of the quadrupole mass spectrometer transmits only a relatively narrow 1–2 eV range of secondary ion energies. Since the secondary ion energy distribution curves have a different shape for the monoatomic ion and for the cluster ions, particularly with the lighter primary ions as described below, the measured ion abundance ratios are distorted relative to true ratios of total ion yields.

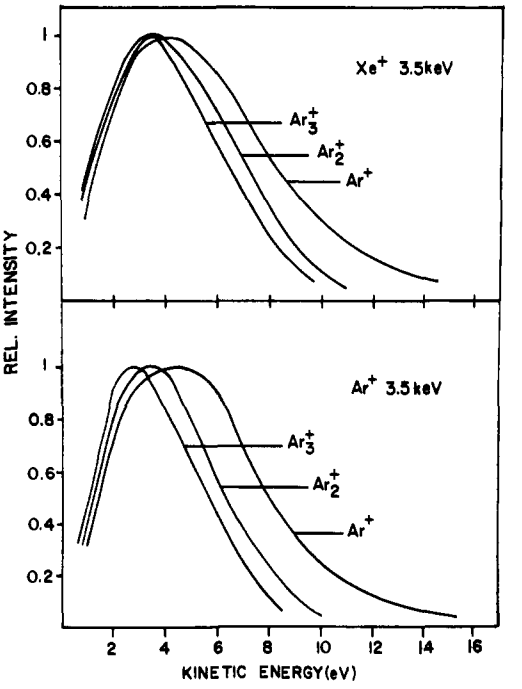

Figure 4. The kinetic energy distribution for the secondary ions Ar^+, Ar_2^+, and Ar_3^+, using (a) Ar^+ (3.5 keV) and (b) Xe^+ (3.5 keV) as the impacting ion.

When He^+, Ne^+, or Ar^+ is the primary ion, the kinetic energy distribution for the secondary ions shows a trend already familiar from previous work on water[10] and alkali halides:[11] the distribution of cluster ions peaks at lower energies than that of the parent ion. Figure 4 shows this trend for Ar^+ as the primary ion and gives the kinetic energy distributions for the secondary ions Ar^+, Ar_2^+, and Ar_3^+. The Ar^+ distribution is broad and has a maximum at about 4 eV, whereas the Ar_2^+ and Ar_3^+ distributions are narrower and have maxima at lower energies, 2.5–3 eV. However, this trend does not continue as the primary ion increases in mass and momentum. As is seen in Figure 4, when Xe^+ is used as the primary ion, the energy distribution of the secondary ions Ar_2^+ and Ar_3^+ is broader than that obtained with Ar^+ as the primary ion, but the distribution of the secondary ion Ar^+ is of comparable width in the two cases. With Xe^+ as the primary ion, the maxima are not as clearly separated as was the case when Ar^+ was the incoming projectile. The behavior of Kr^+ as a primary ion is intermediate between Ar^+ and Xe^+. The kinetic energy distribution of doubly charged secondary ions is the same as that of the singly charged atomic ions.

The primary ions, He^+ to Xe^+, are not observed in the secondary ion spectra, at least not until after some hours of bombardment. This does not contradict our previous observation of ion scattering spectra of low-temperature matrices[6] since the energy filter which has now been incorporated in our instrument will exclude all ions of high energy (over 20 eV), such as those scattered by the surface layer.

A series of SIMS measurements was performed on krypton isolated in a matrix of argon at ratios 1:10, 1:50, 1:100, 1:200, and 1:500. With 3 keV Ar^+ as the primary ion, mixed cluster ions $Ar_nKr_m^+$ were observed to the experimental limit (m/e 1000) in addition to the usual clusters Ar_n^+ and Kr_n^+. With increasing matrix isolation, the relative abundance of clusters containing more than one krypton atom (in both the mixed clusters and the cluster of Kr_n^+) decreased rapidly (Figure 5). At a matrix ratio of 1:500,

(11) F. Honda, G. M. Lancaster, Y. Fukuda, and J. W. Rabalais, *J. Chem. Phys.*, **69**, 4931 (1978).

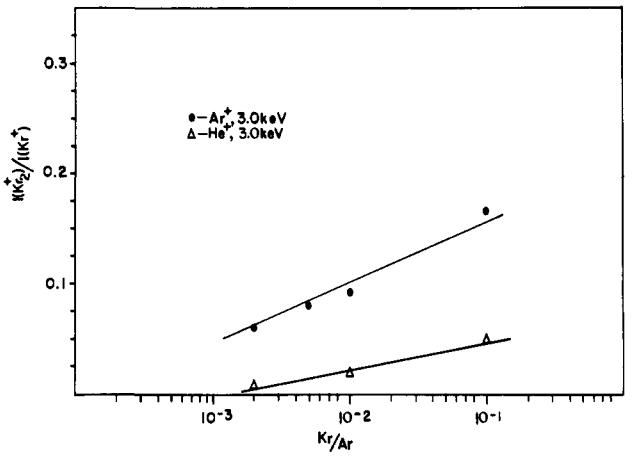

Figure 5. Variation in the intensity ratio of Kr_2^+/Kr^+ as a function of the dilution of Kr in solid Ar matrix, with Ar^+ as the primary ion and He^+ as the primary ion.

the only observed ion which contained more than a single krypton atom was Kr_2^+, and its intensity was only 5% of that of Kr^+.

Several of the measurements at 1:100, 1:200, and 1:500 matrix ratios were repeated with 3 keV and 1 keV He^+ primary ions. In keeping with the results obtained on pure rare gas solids, far fewer clusters were observed, particularly with 1 keV He^+ ions. In the latter case, Ar^{2+}, Ar^+, Ar_2^+, Ar_3^+, $ArKr^+$, and Kr^+ were the only peaks observed already at the 1:100 dilution.

Attempts to observe negative secondary cluster ions from the rare gas solids yielded only negative results.

Discussion

The present results confirm the previous claims[1,5,6,9] that SIMS measurements on molecular solids with very low heats of vaporization and very low sublimation temperatures are feasible. The most striking feature of the spectra is the abundance of rare gas cluster secondary ions formed with the heavier primary projectiles. This is not a serious limitation for matrix-isolation studies, since already with argon the cluster ion peaks are 40 mass units apart and do not block much of the spectrum. Still, it will probably be preferable to use light primary ions such as He^+, for which cluster formation is minimal, and to adjust the energy prefilter to higher kinetic energies in order to further discriminate against them. The rare gas solids appear to be ideal matrices for negative SIMS of matrix-isolated materials.

It appears likely that the observed formation of large cluster ions with the heavier primary projectiles may be used to an advantage and that ion bombardment of rare gas solids will be useful as a source of such ions for studies of their photochemical or collision-induced dissociation and other properties. The properties of cluster ions are currently of considerable interest.[12]

The mechanism of rare gas secondary ion formation and emission is of considerable interest. It is not obvious to what extent it resembles the frequently discussed possible mechanisms for emission of secondary ions from metal surfaces. Among the possibilities most often considered for the latter are the solid fragmentation model[2] and the recombination model.[13] The processes invoked in the former resemble simple "sandblasting" in which small essentially unrearranged pieces of the matrix are ejected attached to a small ion. The processes invoked in the latter involve the ejection of single atoms, molecules, or ions from the bulk of the solid and their recombination in the "selvedge region" in front of the surface, yielding clusters. As a consequence, atoms which were originally not nearest neighbors in the solid may become bonded to each other in the cluster. Experimental support for the occurrence of such processes was obtained in dilution experiments on mixed CsI–KI crystals,[14] and their importance is also indicated by the elemental composition of cluster ions obtained from solids containing polyatomic molecules.[9,10] Theoretical support for the applicability of the recombination model for SIMS of a copper single crystal was obtained from classical trajectory studies.[15] The calculated kinetic energy distribution of secondary ions is narrower and peaks at lower energy for Cu_n^+ clusters than for the Cu^+ ion. This agrees with the experimentally observed behavior of secondary ions from various kinds of solids in previous studies,[1,10,11] and with the present results.

In solids of very low cohesion energy, such as those of interest in the present series of studies, it cannot be excluded that the fracture of the solid into small pieces plays a considerable role. Moreover, it seems possible that reactions and rearrangements within a cluster, as well as partial cluster disintegration, could continue for the whole duration of the flight toward the detector, making an experimental distinction between the fragmentation and recombination models difficult.

As has been discussed previously,[1] the initial formation of ions in the solid can be due to resonant charge transfer, nonresonant charge transfer which involves an inelastic collision between an impacting ion and the target, and inelastic momentum transfer alone. The importance of inelastic momentum transfer is obvious from the appearance of Ar^+ secondary ions in SIMS of solid argon regardless of the nature of the primary projectile: charge transfer to Ar is strongly exothermic from He^+ and Ne^+ but endothermic from Kr^+ and Xe^+, probably even in a solid, as is seen from the following gas-phase appearance potentials (eV): He^+, 24.5; He^{2+}, 54.4; Ne^+, 21.6; Ne^{2+}, 62.6; Ar^+, 15.8 15.9; Ar^{2+}, 43.4; Kr^+, 14.0, 14.7; Kr^{2+}, 38.6; Xe^+, 12.1, 13.4; and Xe^{2+}, 33.3. These numbers show as well that inelastic momentum transfer must also be invoked to account for the formation of the doubly charged secondary ions Ar^{2+}, Kr^{2+}, and Xe^{2+}. We have considered the possibility that their formation is due to doubly charged ions or singly charged metastable ions in the primary beam. This appears extremely unlikely considering the relative intensity of, say, Ar^{2+} relative to Ar^+ obtained with He^+ (0.5 keV) primary ions, which is about 12%, and the fact that electron impact energy used in the ion gun was only 50 eV. The large abundance of doubly charged ions is somewhat surprising considering the relatively slow speed with which they leave the surface and the huge exothermicity of a process in which one of their charges would be transferred to the solid. It is also interesting to note the relative insensitivity of their abundance to the impact energy of the primary projectile contrasted with the great sensitivity to the nature of the primary projectile. A detailed explanation of these observations would require a better understanding of the mechanism of the SIMS process than is currently available.

The reactions which need to be postulated to account for the observed cluster formation in the recombination model are well precedented. The ion–atom association reactions $Ar^+ + 2Ar \rightarrow Ar_2^+ + Ar$ (ref 17) and $Ar_2^+ + 2Ar \rightarrow Ar^{3+} + Ar$ (ref 18) have been studied in detail, and formation of clusters as large as Ar_5^+ has been observed.[19] These reactions and other processes such as $Ar^* + Ar \rightarrow Ar_2^+ + e$, which has been investigated in some detail in the gas phase,[20] may be involved in the SIMS experiments on solid argon. Analogous processes are most likely of importance for the other rare gas solids. Parenthetically, we would like to point out the probable close relation of the processes invoked in SIMS of solid rare gases and small-molecule solids to those ob-

(12) N. Lee, R. G. Keese, and A. W. Castleman, Jr., *J. Colloid Interface Sci.*, **75**, 555 (1980).
(13) N. Winograd, D. E. Harrison, Jr., B. J. Garrison, *Surface Sci.*, **78**, 467 (1980).
(14) F. Honda, Y. Fukuda, and J. W. Rabalais, *J. Chem. Phys.*, *70*, 4834 (1979).
(15) B. J. Garrison, N. Winograd, and D. E. Harrison, Jr., *J. Chem. Phys.*, **69**, 1440 (1978).
(16) J. L. Franklin, et al., *Natl. Stand. Ref. Data. Ser. (U.S., Natl. Bus. Stand.)*, **1969**, 26 (1969).
(17) P. Kebarle, in "Ion-Molecule Reactions", Chapter 7, J. Franklin, *Ed.*, Plenum, New York, 1972.
(18) D. L. Turner and D. C. Conway, *J. Chem. Phys.*, **71**, 1899 (1979).
(19) W. C. Liu and D. C. Conway, Abstracts of the 165th ACS National Meeting, Dallas, Texas, April 9–13, 1973.
(20) K. Radler and J. Berkowitz, *J. Chem. Phys.*, **70**, 221 (1979).

served in radiation chemistry and high-pressure mass spectrometry.[21]

The results obtained on krypton isolated in an argon matrix are highly encouraging. They suggest that even relatively poor matrix isolation ratios such as 1:100 to 1:1000 will be adequate for mass spectrometric investigations of matrix isolated species.

(21) S. G. Lias and P. Ausloos, "Ion-Molecule Reactions, Their Role in Radiation Chemistry", American Chemical Society, Washington, D.C., 1975, p 165.

Acknowledgment. We are grateful to Mr. James A. Thompson-Colón and Mr. Boris Sinković for technical assistance. This work was supported by the National Science Foundation (CHE 78-27094). A part of the vacuum chamber was constructed from material provided by a DOE grant (DE-AC02-79ER10373).

Disilver: Spectroscopy and Photoprocesses in Rare-Gas Matrices

Steven A. Mitchell, Geraldine A. Kenney-Wallace, and Geoffrey A. Ozin*,†

Contribution from the Department of Chemistry, University of Toronto, Toronto, Ontario M5S 1A1, Canada. *Received November 25, 1980*

Abstract: We report the absorption and fluorescence spectra of Ag_2 molecules in Ar, Kr, and Xe matrices at 12 K. A comparison is made with the absorption spectrum of Ag_2 in the gas phase, and detailed assignments of the matrix absorption bands are suggested. The absorption and fluorescence spectra are indicative of strong guest–host interactions involving the $A^1\Sigma_u^+$ and $C^1\Pi_u$ states of Ag_2 in rare-gas matrices. The emission spectrum produced by A–X Ag_2 excitation is interpreted in terms of an excited-state Ag_2 dissociation process, involving strong stabilization of the $^2S + {}^2P$ Ag atomic fragments by matrix cage relaxation effects. Electronic relaxation of the C state of Ag_2 is discussed in terms of matrix cage relaxation, energy transfer to Ag atoms, and nonradiative decay to the A state.

Matrix isolation has proven to be a valuable technique for spectroscopic study of a wide variety of normally unstable metal complexes and molecular metal clusters.[1,2] In particular, matrix trapping and stabilization of silver atoms and clusters have been extensively studied.[3-7] We have recently shown that silver clusters can be formed in a highly controllable manner by photoinduced diffusion and aggregation of matrix-entrapped silver atoms.[8,9] These studies have led to broader enquiries into the nature of electronic relaxation processes of matrix-isolated silver atoms and molecules, with a view to establishing guidelines for the possible extension of the photoinduced diffusion technique to other metal and matrix systems, and to investigate the photoprocesses of matrix-entrapped silver clusters generally.[10,11] In a previous paper[12] we reported the fluorescence excitation, emission, and polarization spectra of silver atoms isolated in Ar, Kr, and Xe matrices, and proposed a qualitative model for the excited-state interactions to account for the observed optical and photolytic properties. In this paper we extend these studies to include fluorescence spectroscopy and electronic relaxation of Ag_2 molecules in rare-gas matrices. The first matrix fluorescence spectrum of Ag_2 was reported by Kolb and Leutloff.[13] We also present a more detailed analysis of our previously reported observations concerning photodissociation of matrix-entrapped Ag_2 molecules.[11]

Laser-induced fluorescence has been used to study the electronic spectra of a wide variety of matrix-isolated diatomic molecules, and to investigate the nature of the guest–host interactions.[14-20] It is often found that the molecular constants are perturbed only slightly in the matrix environment, and in general quite weak guest–host interactions are indicated, although the matrix may influence the electronic relaxation behavior by inducing nonradiative transitions.[21] However, it appears for the case of the excited states of Ag_2 that rather strong guest–host interactions are operative and that unusual electronic relaxation processes are induced by these matrix interactions.

Experimental Section

The experimental arrangement for matrix preparation and fluorescence studies has been described previously.[12] Matrices were deposited onto a NaCl optical window cooled to 12 K by means of an Air Products Displex closed-cycle helium refrigerator. Absorption spectra were re-

Table I. Ag_2 Absorption Maxima in Ar, Kr, and Xe Matrices at 12 K[a]

λ, nm			
Ar	Kr	Xe	gas phase
261 [+720 cm^{-1}]	270 [−557 cm^{-1}]	283 [−2260 cm^{-1}]	266
264	275	289	
(273)	(280)	(296)	
(282)	(290)		
389 [+2720 cm^{-1}]	390 [+2650 cm^{-1}]	391 [+2590 cm^{-1}]	435
(406)			

[a] Absorption maxima due to secondary matrix sites appear in parentheses. The shifts of the major absorption bands from the (0,0) gas-phase transition energies[22,24] are given in square brackets.

† Lash Miller Chemical Laboratories and Erindale College.

(1) G. A. Ozin, *Catal. Rev.-Sci. Eng.*, **16**, 191 (1977).
(2) W. J. Power and G. A. Ozin, *Adv. Inorg. Chem. Radiochem.*, **23**, 79 (1980).
(3) T. Welker and T. P. Martin, *J. Chem. Phys.*, **70**, 5683 (1979).
(4) H. Abe, W. Schulze, and D. M. Kolb, *Chem. Phys. Lett.*, **60**, 208 (1979).
(5) W. Schulze, H. U. Becker, and H. Abe, *Chem., Phys.*, **35**, 177 (1978).
(6) F. Forstmann, D. M. Kolb, D. Leutloff, and W. Schulze, *J. Chem. Phys.*, **66**, 2806 (1977).
(7) W. Schulze, D. M. Kolb, and H. Gerischer, *J. Chem. Soc., Faraday Trans. 2*, **71**, 1763 (1975).
(8) G. A. Ozin and H. Huber, *Inorg. Chem.*, **17**, 155 (1978).
(9) G. A. Ozin, H. Huber, and S. A. Mitchell, *J. Am. Chem. Soc.*, **100**, 6776 (1978).
(10) G. A. Ozin, H. Huber, and S. A. Mitchell, *Inorg. Chem.*, **18**, 2932 (1979).
(11) G. A. Ozin, H. Huber, D. McIntosh, S. Mitchell, J. Norman, Jr., and L. Noodleman, *J. Am. Chem. Soc.*, **101**, 3504 (1979).
(12) S. A. Mitchell, J. Farrell, G. A. Kenny-Wallace, and G. A. Ozin, *J. Am. Chem. Soc.*, **102**, 7702 (1980).
(13) D. Leutloff and D. M. Kolb, *Ber. Bunsenges. Phys. Chem.*, **83**, 666 (1979).
(14) V. E. Bondybey and J. H. English, *J. Chem. Phys.*, **72**, 3113 (1980).

0002-7863/81/1503-6030$01.25/0